JOURNAL OF MATERIALS SCIENCE 33 (1998) 1183–1187

# A new phase in $TiB_2$-reinforced Ni–Al–Fe matrix composite

R. M. WANG*‡, C. H. TAO*, C. Z. LI*, M. G. YAN*
*Beijing Institute of Aeronautical Materials, Beijing 100095, People's Republic of China
‡Beijing Laboratory of Electron Microscopy, Chinese Academy of Sciences, Beijing 100080, People's Republic of China

The microstructure of $TiB_2$-particle-reinforced Ni–Al–Fe matrix composite has been investigated by means of transmission electron microscopy, energy-dispersive X-ray analysis and high-resolution electron microscopy. The dendritic phase is found to be Fe(Ni, Al, Ti), which has a body-centred cubic crystal with lattice parameter $a = 1.068$ nm. High-resolution images indicate that the Fe(Ni, Al, Ti) phase bonds the matrix very well.


## 1. Introduction

The $B_2$ ordered body-centred cubic (b.c.c.) intermetallic compound NiAl is one of the most attractive materials for high-temperature structural applications owing to its low density, high melting point and excellent oxidation resistance, as well as good thermal conductivity [1]. However, the problems of its brittleness at low temperatures and insufficient strength at high temperatures make it difficult for industrial use. The ductility at room temperature has been improved by alloying with Fe [2–4]. One possible approach to increase the elevated-temperature strength is to incorporate metallurgically stable, evenly dispersed, hard and fine second-phase particles in the alloy [5, 6]. Recent studies have shown that the elevated-temperature strength of the NiAl can be obviously improved by dispersively distributed $TiB_2$ or TiC particles fabricated by exothermic dispersion (XD) synthesis [7–9].

There are two different viewpoints on the influence of Fe addition to NiAl intermetallic. One is that the γ-Fe phase covers some boundaries at 750 °C or higher and the α-Fe phase precipitates in the matrix at 500 °C [4]. The other is that FeAl phase particles precipitate with increase in the Fe content. In this paper, a new phase has been found in $TiB_2$-reinforced Ni–Al–Fe matrix composite. The crystal structure of the phase has been identified using conventional transmission electron microscopy (TEM), high-resolution electron microscopy (HREM) and energy-dispersive X-ray spectroscopy.

## 2. Experimental procedure

The XD technique was used to produce Ni–25 at% Al–25 at% Fe *in-situ* composites containing 0–10 vol% $TiB_2$ particles. The reagents used in this research consist of elemental powders of Ni (purity 98%; diameter, less than 28 μm), Al (purity 98%; diameter, less than 13 μm), Ti (purity 99%; diameter, less than 44 μm), Fe (purity 99%; diameter, less than 75 μm) and B. The compression specimen (6 mm × 6 mm × 12 mm) was prepared by electrodischarge machining and grinding. Compression tests were conducted with a MTS810 test machine at the strain rate of $4 \times 10^{-2}\,s^{-1}$.

Specimens for optical microscopy were prepared by conventional procedure, and thin foils for TEM and HREM were prepared by iron milling using 5 kV argon ions in a Gatan dual-ion mill model 600 after dimpling to about 15 μm in the centre. Conventional TEM analysis was performed on an H-800 transmission electron microscope operated at 200 kV. High-resolution images were obtained on a JEOL 2010 microscope with a point-to-point resolution of 0.194 nm at 200 kV. The device for energy-dispersive X-ray analysis (scanning transmission electron microscopy mode) was Oxford Link ISIS 6498 performed on a JEOL 2010 microscope. The calculation software was ISIS version 2.0.

## 3. Results and discussion

The chemical composition of the matrix was chosen as 50 at% Ni, 25 at% Al, 25 at% Fe to improve the ductility of the matrix at room temperature, and the distribution and size of the reinforced particles is controlled.

The XD process relies on the exothermic heat of intermetallic matrix composites. Control of the size of the reinforcement is dependent on the magnitude of the exotherm and the thermal conductivity of the immediate environment. For the $TiB_2$-reinforced NiAl intermetallic composites, the exothermic heat comes from the formation of Ni–Al couples and Ti–B couples. With increase in the contents of the Ti and B powders, the synthetic temperature increases and the $TiB_2$ particles grow larger during the synthesis procedure. However, smaller reinforcements are benefit to the control of the size and distribution of the

particles because they grow larger inevitably in the remelt procedure. On addition of Fe, the Ni–Al couples decrease. Then the synthesis temperature decreases because of the decrease in exothermic heat. Compared with those of NiAl–$TiB_2$ composites, the size of the $TiB_2$ reinforcing particles in (Ni–Al–Fe)–$TiB_2$ composites is reduced obviously. Fig. 1 is an optical micrograph of the (Ni–Al–Fe)–10 vol% $TiB_2$ composites. The $TiB_2$ particles are distributed rather homogeneously in an irregular polygon shape.

Fig. 2 gives a typical bright field of the (Ni–Al–Fe)–$TiB_2$ composites. The $TiB_2$ phase exists in the form of polygonal particles in most cases, and the $TiB_2$ size is in the range 0.1–3 μm. A kind of lamellar or interdendritic structure can be found in the matrix.

Fig. 3 shows the compressive stress-strain curve of the (Ni–Al–Fe) 10 vol% $TiB_2$ composite at room temperature. Compared with that of the NiAl–10 vol% $TiB_2$ composite (8%) [8], the compressive fracture strain of the (Ni–Al–Fe)–$TiB_2$ composite increases to about 20% and the stress strength increases to 997 MPa.

Previous studies have shown that there are at least four kinds of phase in the composites: β-NiAl phase (b.c.c.; $a = 0.288$ nm), γ′-$Ni_3Al$ phase (face-centred cubic (f.c.c.); $a = 0.356$ nm), α-$Al_2O_3$ phase (f.c.c.; $a = 0.79$ nm), $TiB_2$ phase (hexagonal close packed; $a = 0.303$ nm and $c = 0.322$ nm). However, selected electron diffraction indicates that a new phase precipitates in the matrix. Fig. 4 shows a bright-field image of the new phase. The phase is a kind of dendrite. The interdendritic particles are β-NiAl, γ′-$Ni_3Al$ and $TiBi_2$. The selected-area diffraction (SAD) patterns of the dendrite phase are shown in Fig. 5. The measured values for these SAD patterns are shown in Table I. Here $R_1$ and $R_2$ are the shortest and second-shortest vector magnitudes of the two-dimensional reciprocal planes. $d_1$ is the plane spacing corresponding to $R_1$. Θ is the angle between $R_1$ and $R_2$.

Since the group of SAD patterns in Fig. 5 could not be interpreted satisfactorily by any of the known crystal structure in the previous studies, we believe that the dendrite phase in Fig. 4 is a new phase. It is determined that the phase has a f.c.c. crystal structure with lattice parameter $a = 1.068$ nm. Table I also shows the results of which correspond to the SAD patterns in Fig. 5. Here $(h_1\,k_1\,l_1)$ and $(h_2\,k_2\,l_2)$ are the planes corresponding to the two-dimensional reciprocal-lattice vector magnitudes $R_1$ and $R_2$.

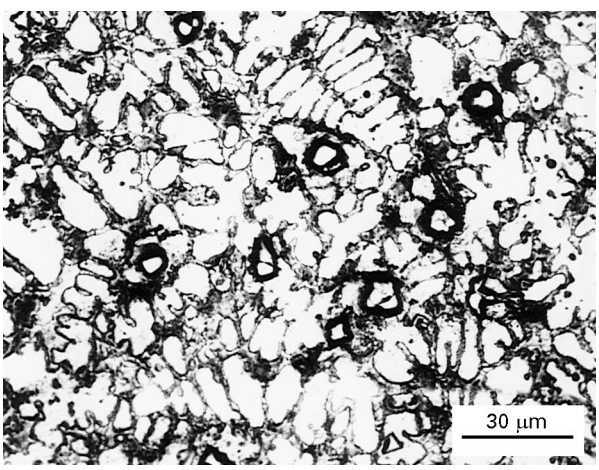


*Figure 1* Metallography of the (Ni–Al–Fe)–$TiB_2$ composites.

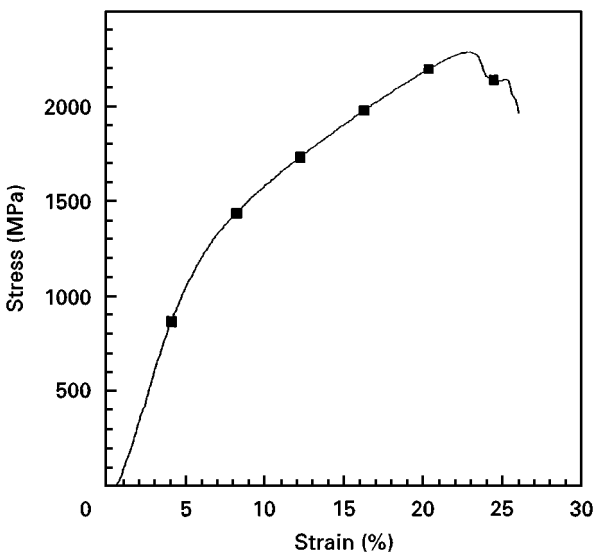


*Figure 3* Compressive stress–strain curve of the (Ni–Al–Fe)–10 vol% $TiB_2$ composite.

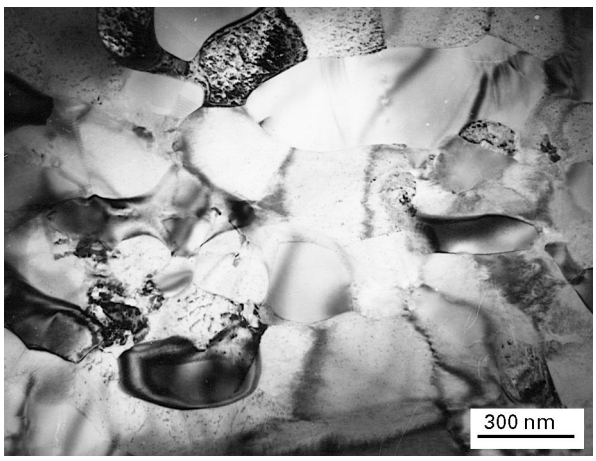


*Figure 2* Bright-field image of the (Ni–Al–Fe)–$TiB_2$ composites.

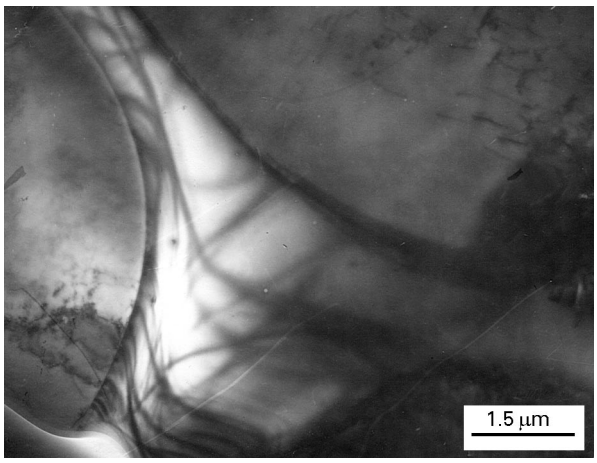


*Figure 4* Bright-field image of the new phase in the matrix.

TABLE I Measured and calculated values of SAD patterns in Fig. 5

| Figure | $R_2/R_1$ | | Θ (deg) | | $d_1$ (nm) | | $(h_1 k_1 l_1)$ | $(h_2 k_2 l_2)$ | $[U V W]$ |
|---|---|---|---|---|---|---|---|---|---|
| | Measured | Calculated | Measured | Calculated | Measured | Calculated | | | |
| 5a | 1.643 | 1.633 | 90 | 90.0 | 0.617 | 0.6166 | $\bar{1}\ \bar{1}\ 1$ | $2\ \bar{2}\ 0$ | 1 1 2 |
| 5b | 2.505 | 2.517 | 98 | 97.61 | 0.617 | 0.6166 | $\bar{1}\ \bar{1}\ 1$ | $3\ \bar{3}\ 1$ | 2 1 3 |
| 5c | 2.525 | 2.517 | 82 | 82.39 | 0.617 | 0.6166 | $\bar{1}\ \bar{1}\ 1$ | $\bar{3}\ 3\ 1$ | 1 2 3 |
| 5d | 1.0 | 1.0 | 66 | 66.42 | 0.240 | 0.2388 | $0\ 4\ \bar{2}$ | $\bar{4}\ 2\ 0$ | 1 2 4 |

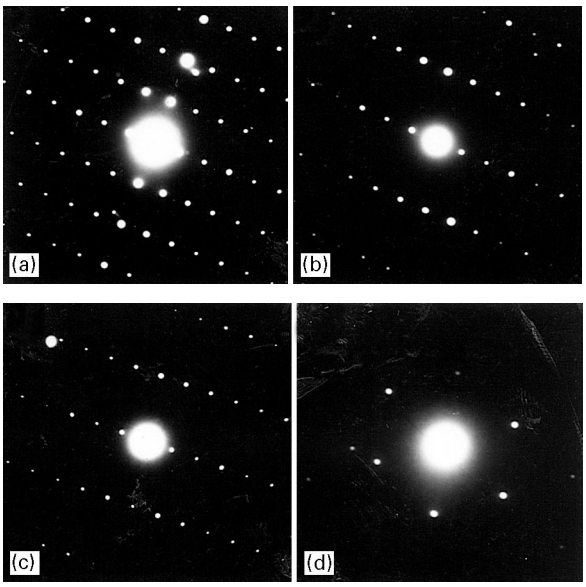


*Figure 5* SAD patterns of Fe(Ni, Al, Ti) phase in Fig. 4.

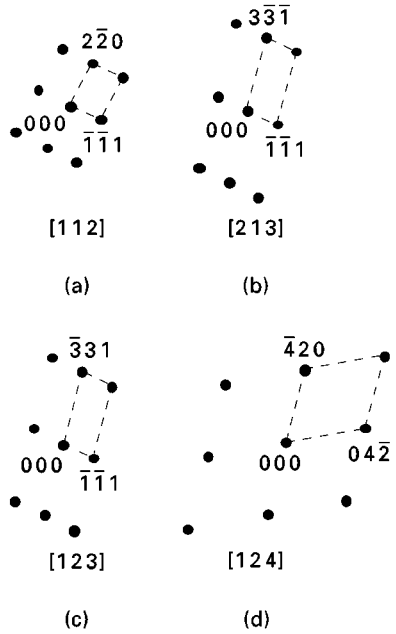


*Figure 6* Indexed SAD patterns of the Fe(Ni, Al, Ti) phase in Fig. 5.

TABLE II Calculated and measured interangles of the SAD patterns in Fig. 5

| Figure | Zone axes | Interangle (deg) | |
|---|---|---|---|
| | | Measured | Calculated |
| 5a and b | [112] and [213] | 11.1 | 10.89 |
| 5b and c | [213] and [123] | − 21.9 | − 21.79 |
| 5c and d | [123] and [124] | − 6.6 | − 7.49 |
| 5d and a | [124] and [112] | 11.7 | 11.49 |

If the above structure of the phase is correct, the calculated angles included between the reciprocal zone axes in Table I should coincide with the corresponding angles measured from the SAD patterns in Fig. 5. This is another way to verify the structure of the phase when measurement errors cannot be avoided. The comparison is shown in Table II. The results are satisfactory.

Fig. 6 is a schematic diagram of the indexed patterns. Fig. 6a, b, c and d correspond to Fig. 5a, b, c and d, respectively.

Fig. 7 gives the energy-dispersive X-ray spectrum of the matrix and the dendrite phase in (Ni–Al–Fe)–$TiB_2$ composite. Many spots have been detected. The spot size of the electron beam varies from 10 to 100 nm owing to the various grain sizes. The chemical composition is summarized in Table III. Despite the fact

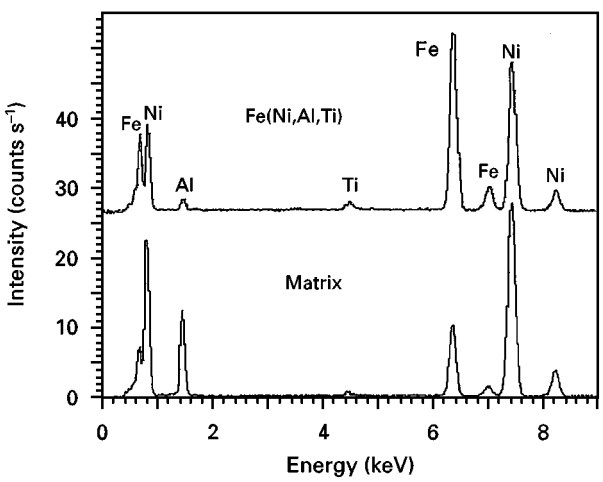


*Figure 7* Energy-dispersive X-ray spectrum of the Fe(Ni, Al, Ti) phase and the matrix.

that the matrix consists of two types of phase (e.g. b.c.c. type and f.c.c. type), the chemical composition of the matrix is found to be almost identical. The chemical content of Ni ranges from 52 to 62 at%. The chemical content range of Al is from 24 to 28 at%. For Fe, the chemical content ranges from 18 to 24 at%. So the matrix can be explained as β-Ni(Al, Fe) and γ′-(Ni, Fe)$_3$Al phases where β-Ni(Al, Fe) has a b.c.c. crystal

TABLE III Chemical composition of the Fe(Ni, Al, Ti) phase and the matrix in (Ni–Al–Fe)–$TiB_2$ composite

| | Amount of the following elements | | | | | | | |
|---|---|---|---|---|---|---|---|---|
| | Al | | Ti | | Fe | | Ni | |
| | (wt%) | (at%) | (wt%) | (at%) | (wt%) | (at%) | (wt%) | (at%) |
| Fe (Ni, Al, Ti) | 1.51 | 3.14 | 1.63 | 1.91 | 49.57 | 49.78 | 47.29 | 45.17 |
| Matrix | 12.40 | 23.31 | — | — | 21.73 | 19.75 | 65.87 | 56.94 |

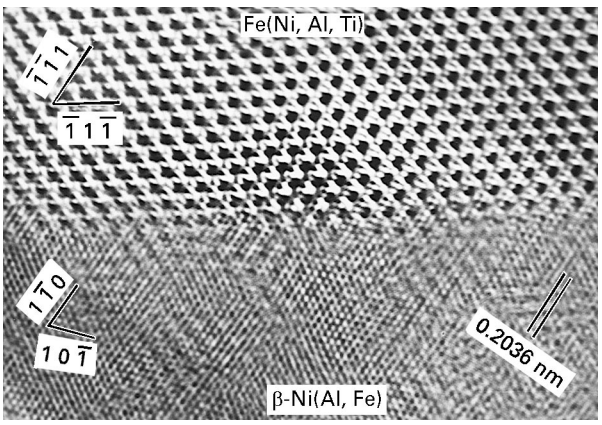


*Figure 8* High-resolution image of the Fe(Ni, Al, Ti)–β-Ni(Al, Fe) interface.

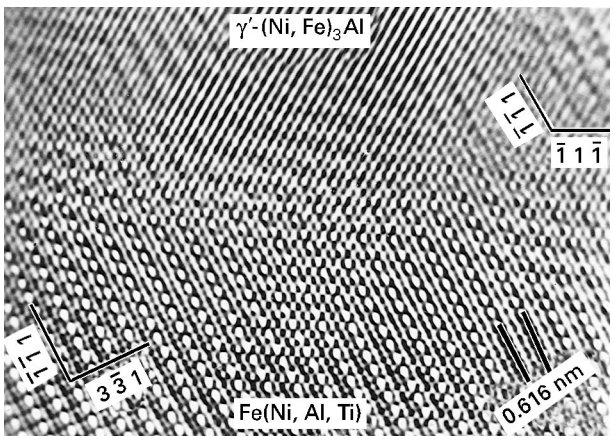


*Figure 9* High-resolution image of Fe(Ni, Al, Ti)–γ′-Ni(Al, Fe) interface.

structure with $a = 0.288$ nm and γ′-(Ni, Fe)$_3$Al has a f.c.c. structure with $a = 0.356$ nm.

From Table I, the chemical content of Fe in the dendrite phase is detected to be about 50 at%. Therefore, the phase may be written as Fe(Ni, Al, Ti).

Investigation shows that no consistent crystallographic orientation relationships were found between the Fe(Ni, Al, Ti) phase and the matrix. Despite this, there are some interesting aspects of interfaces between the Fe(Ni, Al, Ti) phase and the matrix. Fig. 8 shows an high-resolution image of the Fe(Ni, Al, Ti)–β-Ni(Al, Fe) interface. The incident beam is parallel to $[0\,1\,1]_\delta$ and $[1\,1\,1]_\beta$ where δ and β represent the Fe(Ni, Al, Ti) phase and the β-Ni(Al, Fe) phase, respectively. The interface, as indicated by double arrows, is very clean, smooth and straight. No reaction product has been found at the interface. The interplanar spacing of the $(\bar{1}\,1\,\bar{1})$ plane and $(\bar{1}\,\bar{1}\,1)$ plane in the Fe(Ni, Al, Ti) phase are 0.617 nm. The interplanar spacing of the $(1\,\bar{1}\,0)$ plane and $(1\,0\,\bar{1})$ plane in the β-Ni(Al, Fe) phase are 0.204 nm. Fig. 8 gives a semicoherent interface where the interplanar spacing of $(1\,0\,\bar{1})_\beta$ is one third of that of $(\bar{1}\,1\,\bar{1})_\delta$ with a mismatch of about 3%.

Fig. 9 is a high-resolution image of the Fe(Ni, Al, Ti)–γ-(Ni, Fe)$_3$Al interface. The incident beam is parallel to $[1\,2\,3]_\delta$ and $[0\,1\,1]_\gamma$. The interplanar spacings of the $(\bar{1}\,\bar{1}\,1)$ plane and the $(3\,\bar{3}\,1)$ plane in the Fe(Ni, Al, Ti) phase are 0.617 nm and 0.245 nm, respectively. It should also be noted that the two phases have the same types of crystal structure and the lattice parameter of the Fe(Ni, Al, Ti) phase ($a = 1.068$ nm) is just three times that of the γ′-(Ni, Fe)$_3$Al phase. The high-resolution image shows that the interface is clear but not sharp. More high-resolution images indicate that the interface between Fe(Ni, Al, Ti) and γ′-(Ni, Fe)$_3$Al is clear but not sharp. It indicates that the two phases are joined together very well.

## 4. Conclusion

With Ni, Al, Fe, Ti and B elemental powders, Ni–25 at% Al–25 at% Fe matrix composites have been successfully fabricated by the XD technique. The compressive fracture strain increases to about 20% and the stress strength increases to 997 MPa. The $TiB_2$ particles tend to be distributed rather homogeneously with sizes of 0.1 μm. The composites consist of β-N(Al, Fe), γ′-(Ni, Fe)$_3$Al and $TiB_2$ phases as well as the Fe(Ni, Al, Ti) phase. The new Fe(Ni, Al, Ti) phase has a f.c.c. crystal structure with a lattice parameter $a = 1.068$ nm which is just three times that of γ′-(Ni, Fe)$_3$Al. High-resolution images indicate that the Fe(Ni, Al, Ti) phase is well bonded with the matrix and no reaction product is precipitated at the interface. The interface between the Fe(Ni, Al, Ti) phase and β-Ni(Al, Fe) phase is straight while the interface between the Fe(Ni, Al, Ti) phase and γ′-(Ni, Fe)$_3$Al phase is not sharp.

## References


1. R. D. NOEBE, R. R. BOWMAN and M. V. NATHAL, *Int. Mater. Rev.* **38** (1993) 19.
2. A. INOUE and T. MASUMOTO, *J. Mater. Sci.* **19** (1984) 3097.

3. C. T. TSAU, J. W. C. JANG and J. W. YEH, *Mater. Sci. Engng.* **A152** (1992) 264.
4. S. GUHA, I. BAKER, P. R. MUNROE and J. R. MICHAEL, *ibid.* **A152** (1992) 258.
5. K. S. KUMAR and J. K. WHITTENBERGER, *Mater. Sci. Technol.* **8** (1992) 317.
6. L. WANG and R. J. RESENAULT, *Mater. Sci. Engng.* **A127** (1990) 91.
7. *Idem., Metall. Trans.* **A22** (1991) 3013.
8. Z. P. XING, J. Y. DAI, J. T. GUO, G. Y. AN and Z. Q. HU, *Scripta. Metall.* **31** (1994) 1141.
9. Y. X. LU, C. H. TAO and D. Z. YANG, *ibid.* **35** (1996) 1243.

*Received 7 May*
*and accepted 24 September 1997*